



# Double-Coated Poly(butyl Cyanoacrylate) Nanoparticles as a Potential Carrier for Overcoming P-Gp- and BCRP-Mediated Multidrug Resistance in Cancer Cells

Neeraj Kaushal, Zhe-Sheng Chen and Senshang Lin\*

College of Pharmacy and Health Sciences, St. John's University, Queens, NY, United States

## OPEN ACCESS

### Edited by:

René D. Peralta,  
CONACYT Center for Research in  
Applied Chemistry (CIQA), Mexico

### Reviewed by:

Dhiraj Kumar,  
University of Minnesota Twin Cities,  
United States

Qin Jiang,  
Donghua University, China

### \*Correspondence:

Senshang Lin  
linse@stjohns.edu

### Specialty section:

This article was submitted to  
Biomedical Nanotechnology,  
a section of the journal  
Frontiers in Nanotechnology

**Received:** 05 August 2021

**Accepted:** 18 October 2021

**Published:** 28 October 2021

### Citation:

Kaushal N,  
Chen Z-S and Lin S (2021) Double-  
Coated Poly(butyl Cyanoacrylate)  
Nanoparticles as a Potential Carrier for  
Overcoming P-Gp- and BCRP-  
Mediated Multidrug Resistance in  
Cancer Cells.  
*Front. Nanotechnol.* 3:753857.  
doi: 10.3389/fnano.2021.753857

The present study evaluates poly (butyl cyanoacrylate) nanoparticles (PBCA-NPs), double-coated with Tween 80 and polyethylene glycol (PEG) 20,000 as a potential carrier system for overcoming P-glycoprotein (P-gp) and breast cancer resistant protein (BCRP)-mediated multidrug resistance (MDR) in cancer cell lines. Doxorubicin-loaded PBCA-NPs were prepared by the anionic polymerization method and were successively double-coated with Tween 80 and PEG 20000 at varied concentrations. MDR reversing potential was investigated by cellular uptake in P-gp overexpressing cell line. And, the outcomes were verified by modified MTT assay in P-gp or BCRP overexpressing cell lines. The findings from the cell uptake study indicate that double-coated PBCA-NPs significantly enhanced doxorubicin accumulation within the cells. MTT assays revealed that double-coated PBCA-NPs significantly potentiated the sensitivity of doxorubicin in P-gp overexpressing cells, in comparison to free doxorubicin, single-, and un-coated PBCA-NPs, respectively. Moreover, further increase in concentration with Tween 80, double-coated PBCA-NPs significantly enhanced the sensitivity of doxorubicin in BCRP overexpressing cell line, in comparison to single- and double-coated formulations (with lower concentration of Tween 80). Hence, it could be concluded that double-coated PBCA-NPs can be used as a potential carrier for enhancing doxorubicin accumulation in MDR cancer cells.

**Keywords:** doxorubicin, multidrug resistant, nanoparticles, P-glycoprotein (P-gp), transporters, breast cancer resistant protein (BCRP)

## INTRODUCTION

Cancer is characterized by the uncontrolled growth and spread of cancerous cells and remains a major cause of death in the United States, causing over 600,000 fatalities annually. Although with advancement in early detection and advances in chemotherapy have substantially improved the survival rate (i.e., 39% in early 1960s versus 70% currently) (Chemical Society American 2020), acquired multidrug resistant (MDR) unfortunately still imposes a significant obstacle to the success of chemotherapy in many cancers. From a clinical perspective, acquired MDR is described as a phenomenon whereby cancer cells, upon being exposed to one drug, develop cross-resistance to a range of structurally related or unrelated drugs (Gong et al., 2012). Among various reasons, an

overexpression of drug efflux transporters (e.g., P-glycoprotein (P-gp/ABCB1), breast cancer resistant protein (BCRP/ABCG2), etc.) in cell lines has been discussed for describing the MDR phenotype (Wang, Zhang, and Chen 2019). This leads to an elevated efflux of drugs from the cancer cells, subsequently limiting their intracellular accumulation. As a result, this occurrence has been interpreted as an obstacle to the success of chemotherapy (Gottesman, Fojo, and Bates 2002).

Doxorubicin, an anthracycline antibiotic, due to its broad-spectrum efficacy towards multiple cancers, is most widely used chemotherapeutic drug. And, it has been successfully used commercially, when encapsulated within pegylated (“stealth”) liposomes (Doxil®). However, doxorubicin is a substrate for both P-gp and BCRP transporters. Therefore, the major limitation associated with the treatment with Doxil® is the doxorubicin-mediated MDR. For this reason, existing drugs, which are known to inhibit efflux transporters activity (e.g., verapamil and imatinib for P-gp and BCRP transporters, respectively), are co-administered upon initiation of chemotherapy (Summers, Moore, and McAuley 2004; Houghton et al., 2004). Another approach of resolving doxorubicin-mediated MDR would be to identify a novel inhibitor (Jekerle et al., 2006). Nevertheless, such inhibitor may interact with anticancer drug resulting in an altered pharmacokinetics of the anticancer drug (Wandel et al., 1999). To counteract the negative regulation of chemotherapy by efflux transporters, three generations of inhibitors have been developed and some of them have been introduced into clinical trials (Palmeira et al., 2012). However, due to unexpected adverse effects and/or severely drug-drug interaction, none of them have been approved by FDA (Crowley, McDevitt, and Callaghan 2010). Additionally, the translational potential of novel inhibitor from clinic trials to commercial product is a time-consuming and unfavorable economically. This indicates that there is an unmet need for effective and safe reversal agents for clinical use. To overcome these obstacles, polymeric nanoparticles could be used as delivery system for enhancing the accumulation of doxorubicin in acquired-MDR cancer cells (Duan et al., 2012).

In the present study, double-coating approach of poly (butyl cyanoacrylate) nanoparticles (PBCA-NPs) with Tween 80 and PEG 20000 is proposed. An overcoating with Tween 80 for its inhibition action on P-gp transporters has been explored elsewhere (H. Zhang et al., 2003). However, its action on BCRP is not well known. Subsequently, double-coating with polyethylene glycol (PEG) 20,000 plays a substantial role in protecting PBCA-NPs from enzymatic degradation and imparts stealth properties to the PBCA-NPs (Suk et al., 2016). *In-vitro* cell culture is an economical alternative to animal studies. It can aid in understanding the efficacy of the delivery system and its success potential in any future animal studies. Therefore, to evaluate the efficacy of the formulated double-coated doxorubicin-loaded PBCA-NPs for reversing acquired MDR, two pair of cell lines were used. The first one represents the cell line overexpressing P-gp transporters and has acquired resistance towards doxorubicin. For representing acquired MDR trait, the second cell lines represent the overexpression of BCRP transporters acquired by mitoxantrone. In addition,

cellular uptake study and MTT assays were performed to evaluate their effect on doxorubicin-mediated MDR.

## MATERIALS AND METHODS

### Materials

The monomer solution containing n-2-butyl cyanoacrylate (density 0.9580 at 20°C) used for fabrication of the PBCA-NPs was purchased from Glustitch Inc. (Delta, Canada). Doxorubicin hydrochloride [molecular weight (MW) 597.98 Da] (henceforth referred to as doxorubicin) (purity ~99.0%) was purchased from BOCSCI Inc. (Shirley, NY). Dextran 70 (MW 68800 Da), polyethylene glycol (PEG) 20,000, dimethyl sulfoxide, and Whatman® glass microfiber pre-filters (2.5, 0.6 and 0.3 µm) were purchased from VWR International (Radnor, PA). 1X Dulbecco’s phosphate buffered saline (DPBS) was purchased from HyClone™ (Logan, UT). Nanopure® water was used for the preparation of nanoparticles. Super Refined™ polysorbate 80 (Tween 80) was a generous gift from Croda (Edison, NJ). Dulbecco’s modified Eagle’s Medium (DMEM), fetal bovine serum (FBS), penicillin/streptomycin, trypsin 0.25% were purchased from Hyclone (GE Healthcare Life Science, Pittsburgh, PA). All chemicals were of analytical or technical grade and used without further treatment.

### Cell Lines and Cell Culture

The human colon cancer cell line SW620 and its doxorubicin-selected P-gp-overexpressing SW620/Ad300 cells (henceforth referred to as AD300), the NSCLC cell line NCI-H460 and its mitoxantrone-selected BCRP-overexpressing NCI-H460/MX20 cells (henceforth referred to as MX20), were used for P-gp and BCRP reversal study, respectively. All cells were cultured at 37°C, using 5% CO<sub>2</sub> with DMEM containing 10% FBS and 1% penicillin/streptomycin. All drug resistant cell lines were grown as adherent monolayer in a drug-free culture media for more than 2 weeks prior to their use.

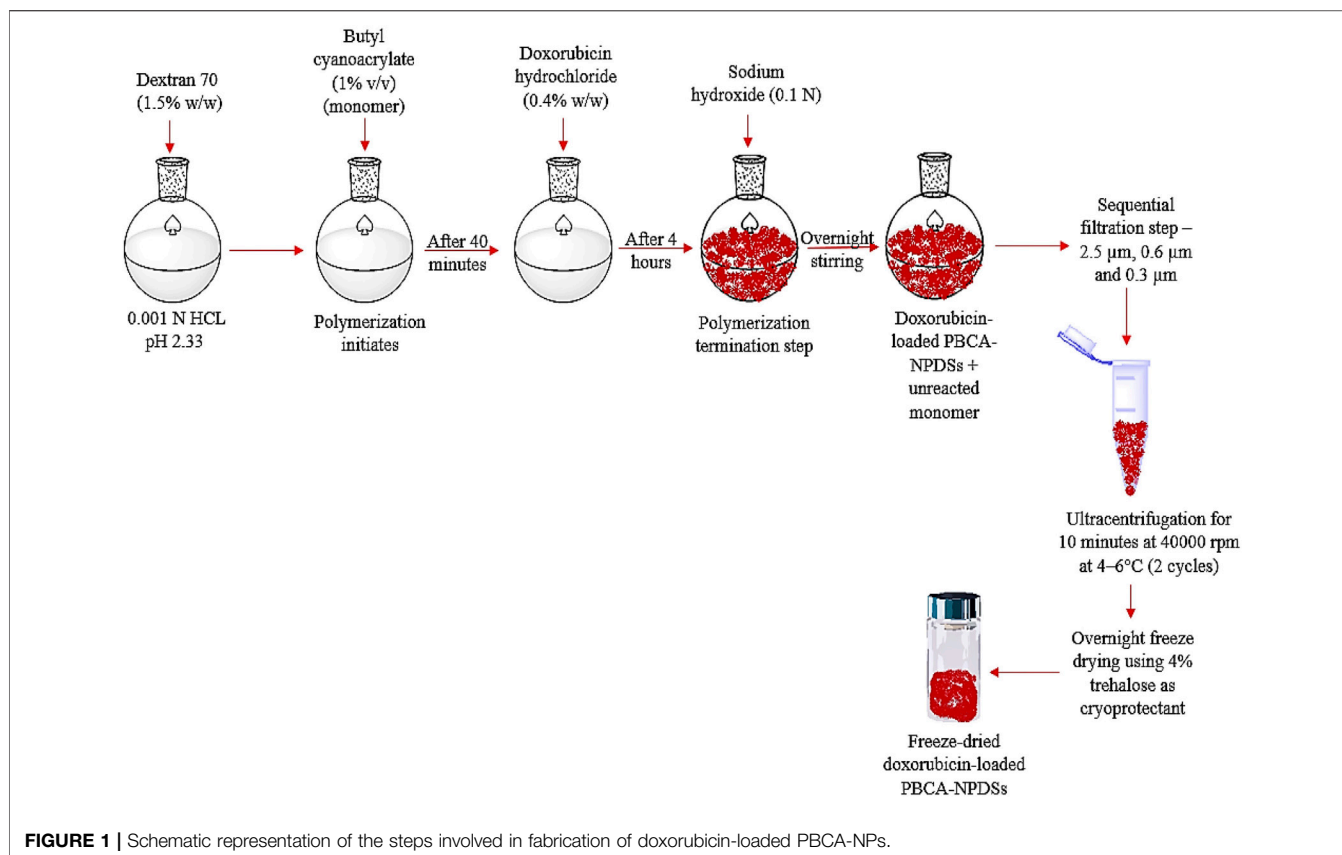
### Analytical Method

#### Analysis of Doxorubicin by UV-Vis Spectroscopy

The doxorubicin content in samples obtained from characterization studies was determined using UV-Vis Spectrophotometer (DU 700 series, Beckman Coulter Inc, Brea, CA) at  $\lambda = 480$  nm (Prados et al., 2015). Serial dilutions of stock doxorubicin solution (1,000 µg/ml) were made to obtain concentrations ranging from 0.1 to 50 µg/ml. Linear regression analysis was performed between the absorbance and the concentration of doxorubicin to establish the calibration curve using SigmaPlot (Systat Software Inc, San Jose, CA).

#### Analysis of Doxorubicin by Fluorescence Microscopy Method

The intracellular accumulation of doxorubicin was studied using fluorescence microscopy reported in the literature (Y.-K. Zhang et al., 2016). Images were collected using EVOS® FL Auto Imaging System (Model AMFAD1000) (Thermo Fisher Scientific, Fair Lawn, NJ). In order to take the images, the cells were visualized at



a total magnification of  $1,200 \times$  ( $40 \times$  objective with an internal magnification of  $30 \times$ ) using two different modes (i.e., phase contrast and fluorescence). Phase contrast was used to locate a region of cells free from any cellular debris and/or any overlapping cells. Fluorescence was used to determine doxorubicin accumulation within the cells, which was achieved by selecting the RFP filter (built-in the instrument) at a preset wavelength (excitation: 552 nm; emission: 585 nm). For both phase contrast as well as fluorescence, images of cells were acquired using a monochrome camera also built-in the instrument.

### Fabrication of Double-Coated Doxorubicin-Loaded PBCA-NPs

The doxorubicin-loaded PBCA-NPs were prepared by an anionic polymerization method with modifications as reported (Gulyaev et al., 1999) and schematically represented in **Figure 1**. Briefly, dextran 70 (1.5% w/w, i.e., 1.5 g) was added to 100 ml 0.001 N HCl solution (pH  $\sim 3.00$ ) under constant magnetic stirring at low speed (500–800 rpm) with a Pyrex<sup>®</sup> Spinbar<sup>®</sup> (VWR International, Radnor, PA). Once dextran 70 was completely solubilized, butyl cyanoacrylate monomer solution (1% v/v, i.e., 1 ml) was added dropwise. After 40 min of polymerization, 20 ml doxorubicin (0.4% w/v in 0.001 N HCl) was then added. Following 4 h of polymerization, the reaction mixture was

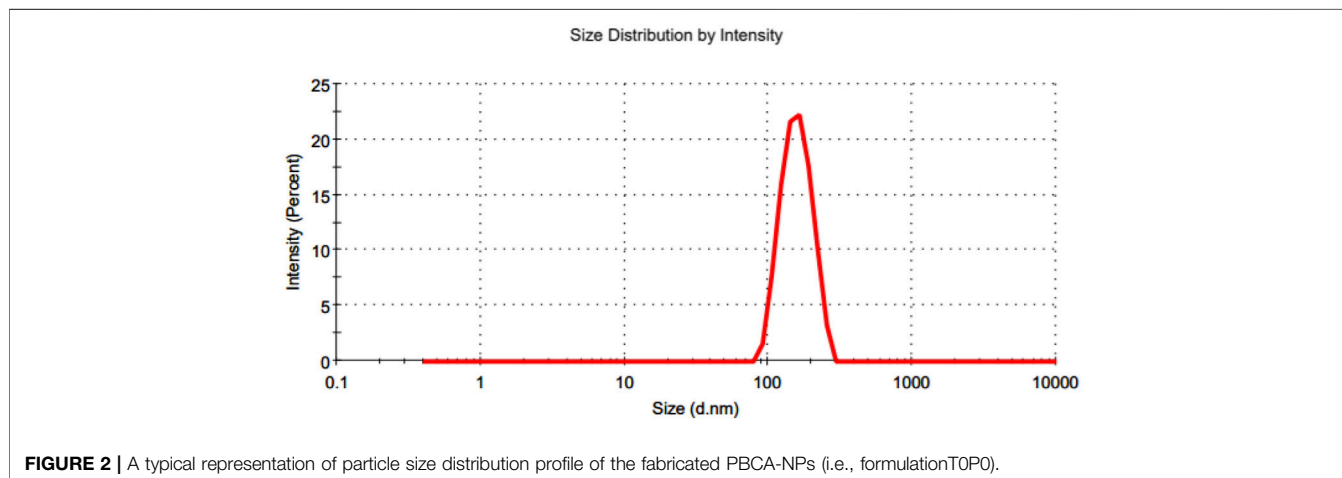
further added dropwise with sodium hydroxide (0.1 N) till pH 6.8–7.0 to terminate polymerization reaction by neutralizing the solution. This was performed via titration method while continuously monitoring the pH solution under constant stirring using a digital pH meter. Thereafter, the reaction mixture was further stirred for an additional 12 h to ensure complete neutralization. The nanoparticle suspension obtained was then subjected to sequential filtration step using 2.5, 0.6, and 0.3  $\mu\text{m}$  filters with a vacuum filtration assembly. The filtered suspension was further subjected to ultracentrifugation for two cycles (10 min each at 40,000 rpm and 4–6°C) using Optima XE ultracentrifuge, rotor Type 70 Ti (Beckman Coulter, Indianapolis, IN). After each centrifugation step, the supernatant was removed, and the nanoparticles were resuspended in the same amount of Nanopure<sup>®</sup> water using brief sonication. Finally, the pelleted nanoparticles were immediately frozen using a freezing mixture of dry ice and alcohol. The frozen nanoparticles were then immediately lyophilized using a Freezone 4.5 lyophilizer (Labconco, Kansas City, MO). Lyophilization was carried out at  $-51^\circ\text{C}$  and at a pressure of 0.018 mbar in the presence of 4% trehalose as a cryoprotectant overnight and then stored at 2–8°C until further use.

The doxorubicin-loaded PBCA-NPs were coated successively with varying concentrations of up to 2% of Tween 80 and PEG 20000 relative to the total suspension volume of nanoparticles

**TABLE 1** | Formulation codes and characteristics of various doxorubicin-loaded PBCA-NPs formulations (data present mean  $\pm$  SD,  $n = 3$ ).

Formulation	Code	Particle size (nm)	PdI	Zeta potential (mV)	Entrapment efficiency (%)
—	Placebo <sup>a</sup>	109.4 $\pm$ 3.3	0.083 $\pm$ 0.022	-3.09 $\pm$ 0.97	Not applicable
Core	T0P0	154.5 $\pm$ 1.4	0.044 $\pm$ 0.039	3.13 $\pm$ 0.84	89.9 $\pm$ 0.1
Single-coated	T0P1	182.6 $\pm$ 25.5	0.040 $\pm$ 0.019	2.72 $\pm$ 0.94	87.0 $\pm$ 0.1
	T1P0	154.4 $\pm$ 5.7	0.076 $\pm$ 0.028	4.19 $\pm$ 0.78	88.3 $\pm$ 0.3
Double-coated	T1P1	203.6 $\pm$ 8.1	0.064 $\pm$ 0.046	5.29 $\pm$ 2.24	88.5 $\pm$ 0.1
	T1P2	256.9 $\pm$ 9.1	0.082 $\pm$ 0.017	3.95 $\pm$ 0.84	88.5 $\pm$ 0.4
	T2P1	221.0 $\pm$ 20.0	0.129 $\pm$ 0.116	3.08 $\pm$ 2.30	86.5 $\pm$ 0.2
	T2P2	276.2 $\pm$ 15.4	0.110 $\pm$ 0.062	2.75 $\pm$ 0.48	88.4 $\pm$ 0.3

<sup>a</sup>Placebo: PBCA-NPs (blank nanoparticles).



(Das and Lin 2005). For each formulation, required quantities of Tween and/or PEG were added stepwise in the above suspension. This suspension was then kept in a water-shaker bath, maintained at  $25 \pm 0.5$  °C and 100–120 cycles per min for 90 min. For convenience in terminology, based on the amount of coating of Tween 80 and PEG 20000 different formulations were coded. For example, as displayed in **Table 1**, T1P1 represents 1% of Tween 80 and 1% PEG 20000.

### Characterizations of Double-Coated Doxorubicin-Loaded PBCA-NPs Particle Size and Zeta Potential

All double-coated doxorubicin-loaded PBCA-NPs formulations (5 mg) were suspended in 1 ml DPBS by brief sonication. This homogenous suspension was then transferred to a folded capillary cell (DTS1070) (Malvern Panalytical Inc. Westborough, MA). After a brief equilibration period inside the sample chamber, the mean hydrodynamic particle size (nm), the polydispersity of size distribution (PdI) and zeta potential were measured. For particle size analysis, dynamic light scattering (DLS) along with Non-Invasive Back Scatter Technology built-in the Zetasizer Nano ZS (Malvern Panalytical Inc. Westborough, MA) was used. Zeta potential

was measured using laser doppler micro-electrophoresis also built-in the Zetasizer Nano ZS. The fundamental size distribution generated by DLS is an intensity distribution, which can be converted to a volume distribution. This volume distribution can also be further converted to a number distribution. However, number distributions are of limited use as small errors in gathering data for the correlation function which may lead to huge errors in distribution by number. Therefore, the particle size graph representing an intensity distribution was chosen for data interpretation. In addition, it may be worthwhile to note that various parameters (e.g., viscosity, refractive index, dielectric constant of the tested samples) can impact both the particle size and zeta potential measurements of the fabricated nanoparticles. However, impact of these parameters is not performed for routine analysis. Most often a suitable buffer system representative of a suitable diluent is selected to understand the characteristics of these nanoparticles. Since DPBS solution in water does not absorb (i.e., absorption coefficient practically equal to 0) the usual wavelengths of the lasers used in DLS (500–780 nm). At a given wavelength, not concentrated solutions of Pi buffer have the same refractive index as water. Therefore, 0.8872 cP, 1.330 (dimensionless), 78.4 (dimensionless), respectively, for viscosity, refractive index and dielectric constant of water were used as

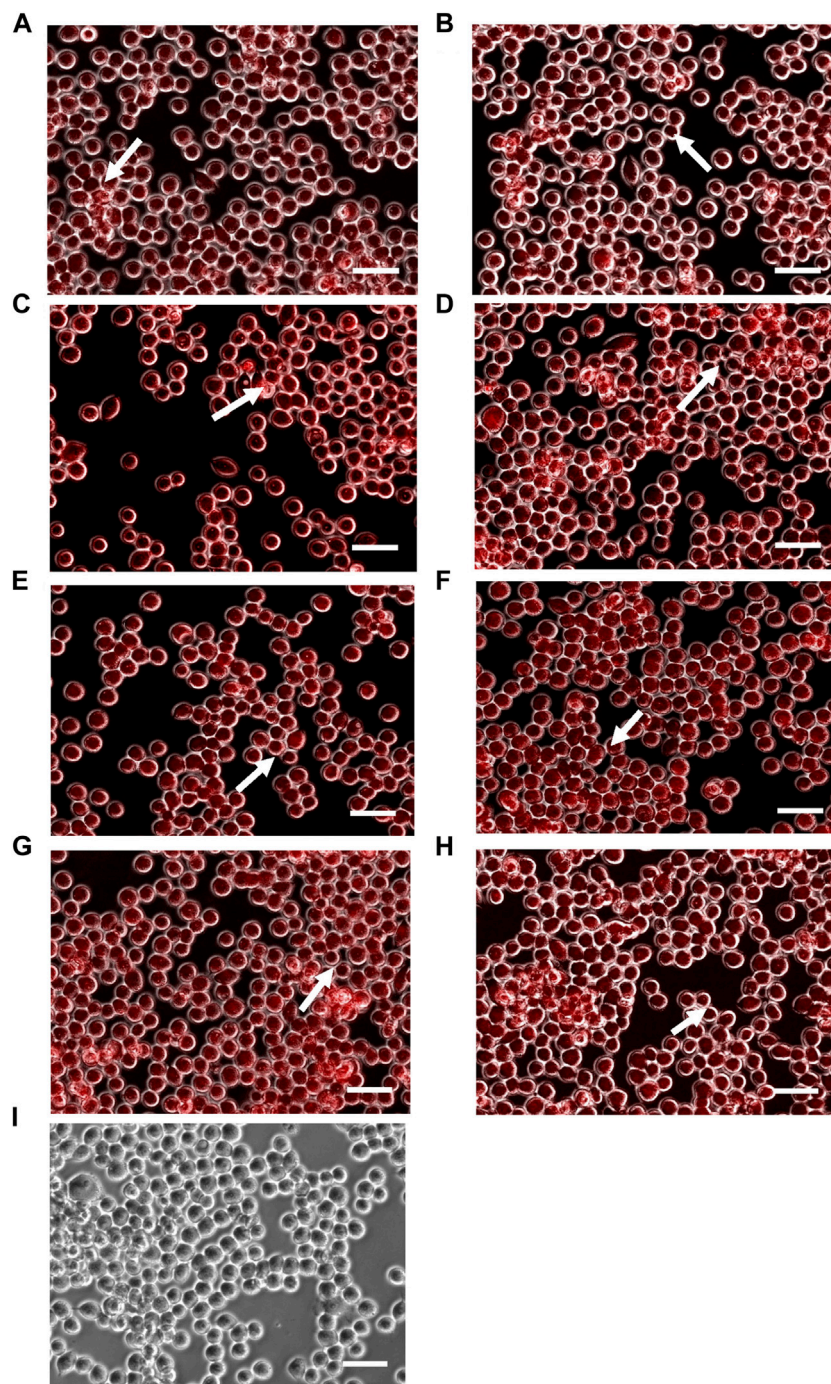


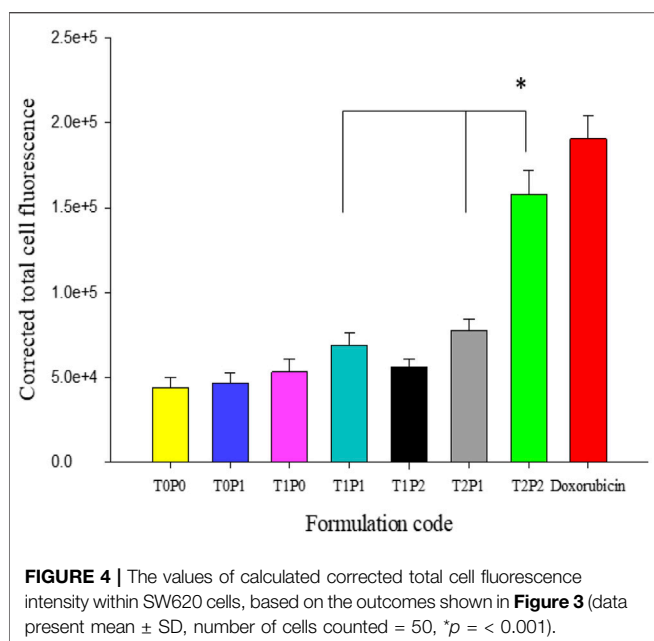
**FIGURE 3** | Intracellular accumulation of doxorubicin within SW620 cells, following treatment with formulations **(A)** T0P0, **(B)** T0P1, **(C)** T1P0, **(D)** T1P1 **(E)** T1P2, **(F)** T2P1, **(G)** T2P2 as well as **(H)** doxorubicin solution and **(I)** no treatment (as control groups). Arrows represents accumulation of doxorubicin in the nucleus (magnification:  $\times 10$ , scale bar: 10  $\mu\text{m}$ ).

default reference values of equipment during these measurements.

### Entrapment Efficiency

The amount of drug entrapped was determined by completely dissolving the lyophilized doxorubicin-loaded PBCA-NPs (5 mg)

in 5 ml methanol:acetonitrile (50:50) solution. The resulting solution was centrifuged at 13,300 rpm for 10 min at  $4 \pm 0.5^\circ\text{C}$  to pelletize any undissolved materials. The clear supernatant was analyzed for doxorubicin content by the UV-Vis spectroscopy method described previously. The entrapment efficiency of doxorubicin was then calculated as a ratio of the assayed



doxorubicin in lyophilized doxorubicin-loaded PBCA-NPs to the total doxorubicin (i.e., 400 mg) used in the fabrication as reported in the literature (Papadimitriou and Bikiaris 2009).

### ***In-vitro* cell culture studies of double-coated doxorubicin-loaded PBCA-NPs**

#### **Intracellular Accumulation Study in SW620 and AD300 Cell Lines**

SW620 and AD300 were seeded in their respective growth medium in 24-well plate and cells were allowed to grow overnight at 37°C, 5% CO<sub>2</sub>. On the day of the experiment, cells were washed with DPBS (pH 7.4) three times. Subsequently, the cells were treated with 5  $\mu$ M free doxorubicin in solution (medium: DPBS without FBS), all double-coated doxorubicin-loaded PBCA-NPs formulations (equivalent to 5  $\mu$ M doxorubicin), and blank (growth mediums). The treated cells were then incubated for 2 h at 37°C, 5% CO<sub>2</sub>. Since it is widely reported that FBS is likely to interfere with the formulations diluted to desired concentration with DPBS without FBS. Without FBS the cells have a very limited lifeline, which according to literatures is between 2 and 4 h. Therefore, to avoid any interference from such factors, 2 h time-point was chosen for intracellular accumulation studies. Following the incubation period, the treatment (free drug, double-coated doxorubicin-loaded PBCA-NPs formulations, or growth medium) was aspirated. The cells were gently washed with DPBS three times and then immediately examined the cells using the fluorescence microscopy method described previously. For this study, single-coated formulations, free doxorubicin, and growth medium served as controls.

Since it is difficult to estimate the amount of up taken doxorubicin from microscopic images, an empirical parameter

[i.e., corrected total cell fluorescence (CTCF)], expressed as fluorescence intensity, was chosen for indirect quantification of doxorubicin within the cell (Jensen 2013). CTCF was obtained after subtracting the intensity of the blank cells (background) from cells exhibiting fluorescence. This was performed using ImageJ<sup>®</sup> software (National Institutes of Health, Bethesda, MD). Higher fluorescence intensity was used as a surrogate for higher intracellular accumulation of doxorubicin.

#### **Cytotoxicity Determination to Evaluate Their P-Gp and BCRP Efflux Transporter Inhibition Potential**

The modified paraformaldehyde, 3-(4,5-dimethylthiazol-2-yl)-2,5-diphenyl-tetrazolium bromide (MTT) colorimetric assay was used to detect the sensitivity of cells to doxorubicin as well as double-coated doxorubicin-loaded PBCA-NPs *in vitro* (Y.-K. Zhang et al., 2015). A general procedure followed for all cell lines used in this investigation has been described (Y.-K. Zhang et al., 2015). Briefly, cells were loaded in 180  $\mu$ l of complete growth medium in 96-well plates in triplicate at cell density of 5,000–6,000 cells/well. After incubation at 37°C, 5% CO<sub>2</sub> for 24 h, cells were treated with different concentrations of doxorubicin solution or double-coated doxorubicin-loaded PBCA-NPs (20  $\mu$ l/well). After 72 h incubation at 37°C, 5% CO<sub>2</sub>, 20  $\mu$ l of MTT solution (4 mg/ml) was added to each well. The plates were further incubated at 37°C, 5% CO<sub>2</sub> for 4 h, enabling viable cells to change the yellow-colored MTT into dark-blue formazan crystals. Subsequently, the MTT/medium was carefully aspirated from each well without disturbing the cell, and 100  $\mu$ l of DMSO was added into each well. Plates were placed on shaking table to ensure thorough mixing of formazan into DMSO. Finally, the absorbance was determined at 570 nm using microplate reader (ThermoFisher Scientific, Waltham, MA) and data acquisition was performed by SkanIt<sup>™</sup> software (ThermoFisher Scientific).

#### **Statistical Analysis**

All the acquired data were expressed as mean  $\pm$  standard deviation (SD), and analyzed with SigmaStat (Systat Software Inc, San Jose, CA). Differences between multiple groups were evaluated by one-way analysis of variance (ANOVA) followed by Holm-Sidak post-hoc analysis to determine the groups, which showed significant difference. In each case, a  $p$ -value less than 0.05 was considered as a representation of significant difference.

## **RESULTS AND DISCUSSION**

### **Analytical Methodology**

The absorbance, measured using both the UV-Vis and fluorescence spectroscopy methods, was found to increase linearly with the increasing concentration of doxorubicin within the measured concentration range with a regression coefficient ( $R^2$ ) value of more than 0.995. These results indicate that both the UV-Vis and fluorescence spectroscopy methods, adopted for the detection and quantification of doxorubicin, are reliable methods.

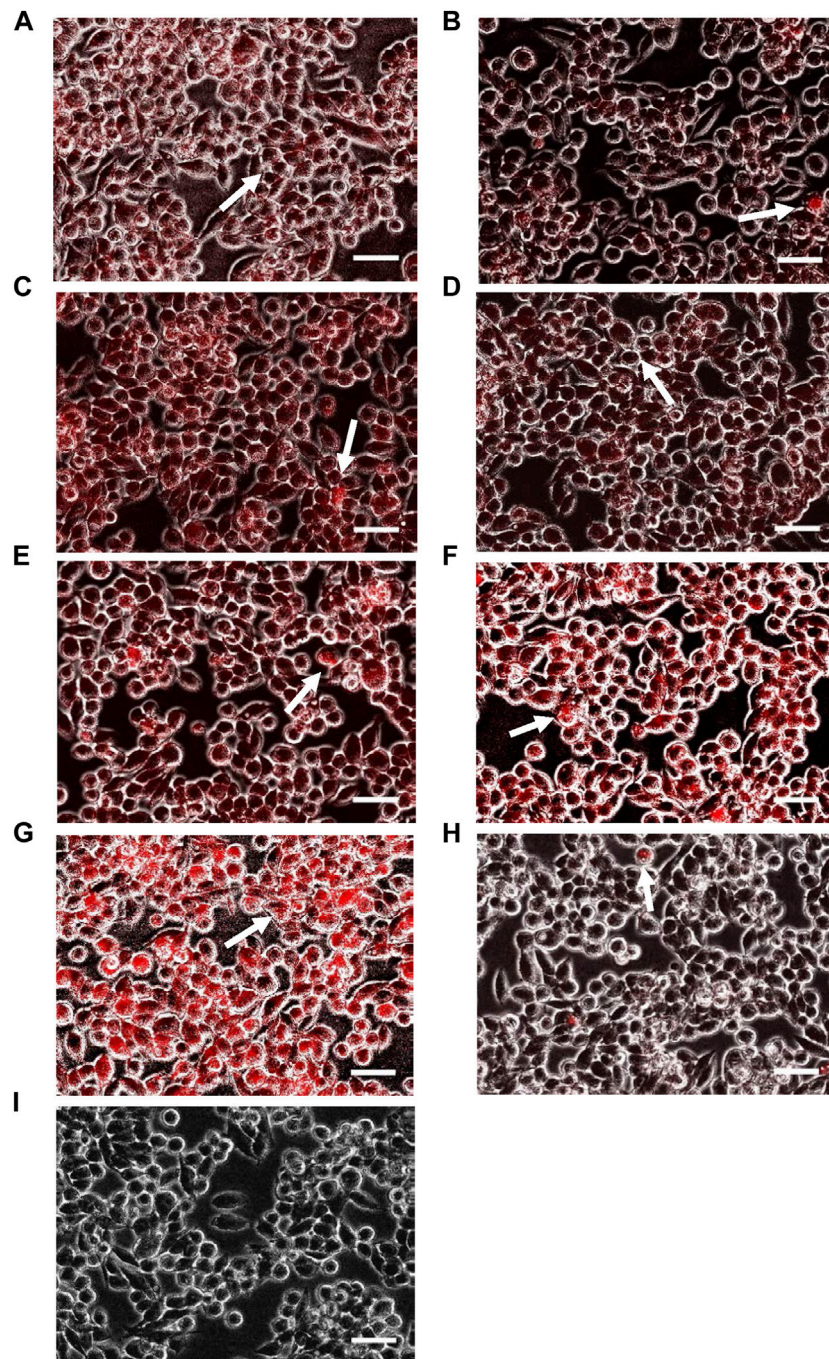
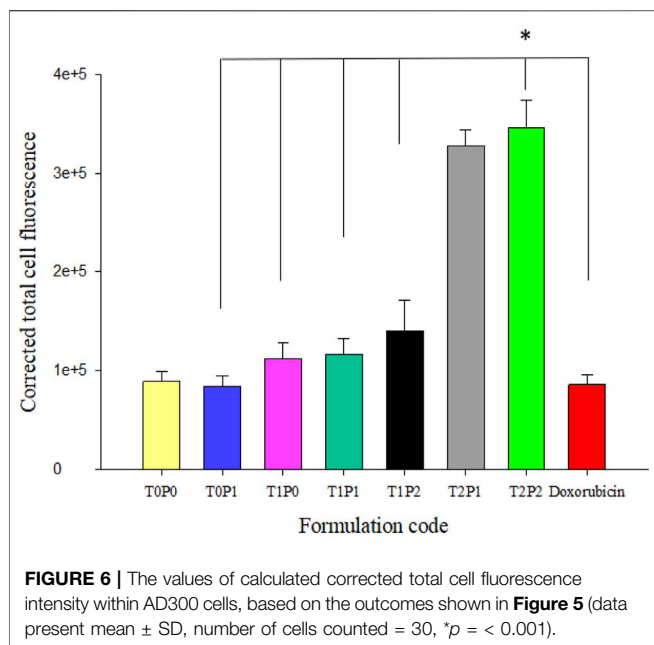


**FIGURE 5** | Intracellular accumulation of doxorubicin within AD300 cells, following treatment with formulations **(A)** T0P0, **(B)** T0P1, **(C)** T1P0, **(D)** T1P1 **(E)** T1P2, **(F)** T2P1, **(G)** T2P2 as well as **(H)** doxorubicin solution and **(I)** no treatment (as control groups). Arrows represents accumulation of doxorubicin in the nucleus (magnification:  $\times 10$ , scale bar:  $10\ \mu\text{m}$ ).



## Characterization of Double-Coated Doxorubicin-Loaded PBCA-NPs

### Particle Size, Zeta Potential and Entrapment Efficiency

The particle size, polydispersity index (PDI), zeta potential and entrapment efficiency of various non-coated and coated doxorubicin-loaded PBCA-NPs formulations in comparison with blank PBCA-NPs nanoparticles (placebo) are summarized in **Table 1**. And, a typical particle size distribution profile of fabricated PBCA-NPs (i.e., formulation T0P0) is shown in **Figure 2**.

As expected, the mean particle size of doxorubicin-loaded PBCA-NPs (formulation T0P0) increased, due to doxorubicin loading, as compared to that of blank PBCA-NPs (154.5 versus 109.4 nm). This increase in size could be attributed to interference in the surface deposition of dextran 70 (surfactant) chains caused by the presence of doxorubicin during the polymerization step. As a result, their adsorption on the PBCA-NPs may have reduced, leading to an increase in the particle size as reported elsewhere (Vansnick et al., 1985). Further coating of doxorubicin-loaded PBCA-NPs with Tween 80 and PEG 20000 at 1%, respectively, the mean particle size of single-coated doxorubicin-loaded PBCA-NPs increased to 182.6 nm (formulation T0P1) or remained similar size at 154.4 nm (formulation T1P0). This could be attributed to the high MW of PEGs (MW > 5,000 Da) resulted in the formation of a layer-wise polymeric network on the surface of PBCA-NPs (Chognot et al., 2003). Furthermore, with double coating with Tween 80 at 1% and PEG 20000 at either 1% or 2%, mean particle size of the double-coated formulations increased from 154.4 nm (formulation T1P0) to 203.6 nm (formulation T1P1) and 256.9 nm (formulation T1P2). In addition, with double coating with Tween 80 at either 1% or 2% and PEG 20000 at 1%, mean particle size of the double-coated formulations increased

from 182.6 nm (formulation T0P1) to 203.6 nm (formulation T1P1) and 221.0 nm (formulation T2P1). Finally, with double coating with Tween 80 and PEG 20000 up to 2%, mean particle size of the double-coated formulations increased from 154.5 nm (formulation T0P0) to 203.6 nm (formulation T1P1) and 276.2 nm (formulation T2P2). This could be attributed to the presence of Tween 80 facilitating the hydrogen bond formation with incoming PEG 20000 as a double coating, forming a layer-wise coherent coating over doxorubicin-loaded PBCA-NPs (Tejwani et al., 2000). On the other hand, the mean particle size slightly increased from 256.9 nm (formulation T1P2) to 276.2 nm (formulation T2P2). Therefore, it can be concluded that an overcoating with high molecular weight of PEG may impact the particle size of doxorubicin-loaded PBCA-NPs. PDI (a dimensionless quantity) is basically a representation of the particle size distribution of nanoparticles within a given sample population. All formulations (**Table 1**) exhibited low PDI values (< 0.2), this could be attributed to serial filtration step employed during the preparation and isolation of nanoparticles from reaction medium. A low PDI ( $\leq 0.2$ ) is generally deemed acceptable particle size distribution of nanoparticles when selecting polymeric nanoparticles as a delivery system (Danaei et al., 2018).

The mean zeta potential of blank PBCA-NPs was observed to be -3.09 mV (**Table 1**). This inherent -ve zeta potential could be due to the resonance stabilized negative charge formed during the polymerization step (Duffy, Zetterlund, and Aldabbagh 2018). Interestingly, the zeta potential of uncoated doxorubicin loaded PBCA-NPs (formulation T0P0) showed a positive shift in zeta potential following the addition of doxorubicin as compared to the blank PBCA-NPs (3.13 mV versus -3.09 mV). This shift in the zeta potential of formulations could be attributed to the predominant positive charge of doxorubicin (pKa = 8.2) at a pH of 3.00 used during the polymerization reaction. For various doxorubicin-loaded PBCA-NPs formulations, zeta potential values varied from 2.72 mV (formulation T0P1) to 5.29 mV (formulation T1P1). No obvious trend in mean zeta potential values as a result of single- or double-coating was observed. These findings suggest that the coating did not impact the shear plane of the particle, which otherwise would have resulted in shifts in zeta potential values.

As displayed in **Table 1**, the entrapment efficiency of doxorubicin within the various doxorubicin-loaded PBCA-NPs formulations varied from 86.5% (formulation T2P1) to 89.9% (formulation T0P0). This could be attributed to adding doxorubicin during the polymerization step. Doxorubicin added during the polymerization step may act as a nucleophile and can form a part of the growing polymeric chain, yielding higher entrapment within the formed nanoparticles (Kreuter 1994). All formulations evaluated in this study have a polymeric matrix which was stored as freeze dried particles and hence are stable for long duration. Moreover, all formulations (except placebo) were slightly + ve (**Table 1**), when measured in DPBS (pH 7.4), since the cell culture medium also has a pH of 7.4, the zeta-potential is not likely to change. Therefore, nanoparticle-cell interaction is not likely to get impacted.



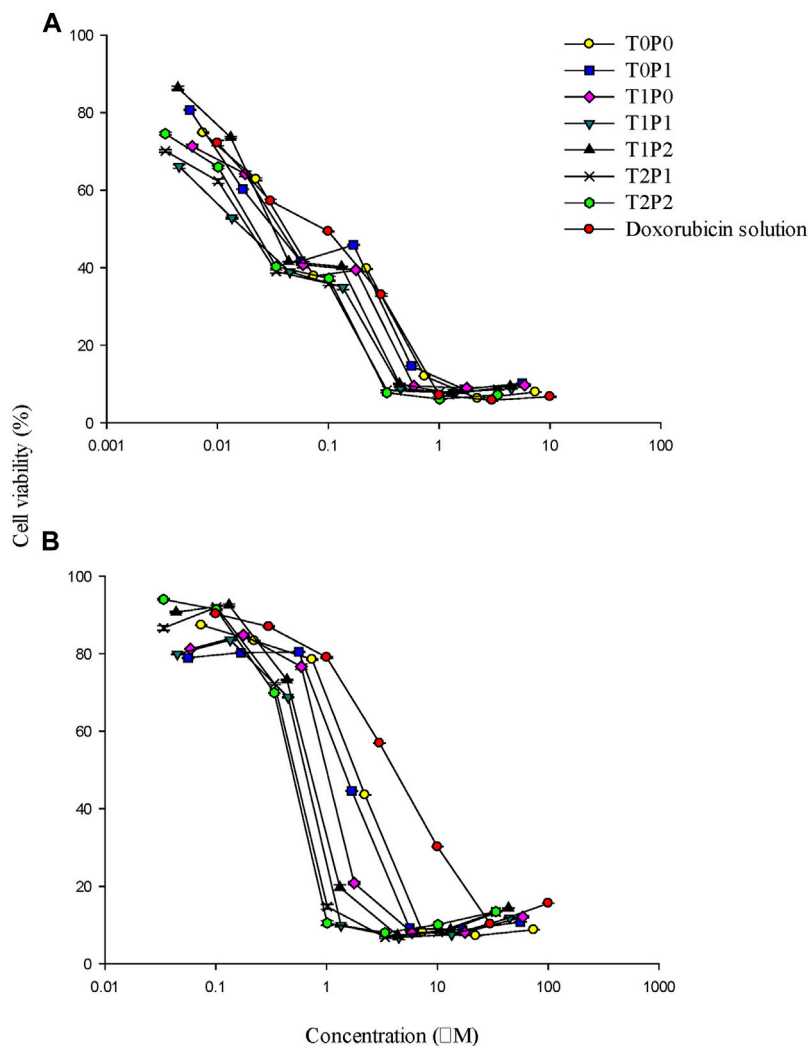


**FIGURE 7** | The cytotoxicity profiles of doxorubicin-loaded PBCA-NPs formulations from MTT assays performed on **(A)** SW620 and **(B)** AD300 cell lines (data present mean  $\pm$  SD,  $n = 3$ ).

### ***In-vitro* Cell Culture Studies of Double-Coated Doxorubicin-Loaded PBCA-NPs**

#### ***Intracellular Accumulation Study in SW620 and AD300 Cell Lines***

To investigate the uptake of double-coated doxorubicin-loaded PBCA-NPs, intracellular accumulation of doxorubicin within SW620 cells, based on its characteristic red fluorescence, was determined, and shown in **Figure 3**. And, for the comparison of outcomes shown in **Figure 3**, the corresponding corrected total cell fluorescence values, were calculated and represented in **Figure 4**.

As shown in **Figure 3**, doxorubicin-associated fluorescence occurred mainly in the nuclei of the SW620 cell line for all doxorubicin-loaded PBCA-NPs formulations (**Figures 3A–G**) and free doxorubicin (**Figure 3H**). Based on the calculated corrected total cell fluorescence values shown in **Figure 4**, a

trend of increase in mean fluorescence intensity with an increase in the concentration of Tween 80 was observed. Formulation T2P2 significantly increased ( $p < 0.001$ ) increased the accumulation of doxorubicin in comparison to formulations T1P1 and T2P1. Furthermore, no significant difference was observed in the fluorescence intensity between formulation T2P2 and free doxorubicin solution. This finding could be attributed to the sensitivity of the cell line toward treatment with doxorubicin. Since SW620 cells do not overexpress P-gp transporters, doxorubicin could readily access the cells and the rate of drug efflux is also reduced.

In addition to the SW620 cell line, intracellular accumulation of various doxorubicin-loaded PBCA-NPs formulations were performed with the AD300 cell line. The characteristic red fluorescence and corresponding corrected total cell fluorescence values are shown in **Figures 5, 6** respectively.

**TABLE 2 |** The IC<sub>50</sub> values calculated from cytotoxicity profiles doxorubicin-loaded PBCA-NPs formulations from MTT assays performed on SW620 and AD300 cell lines (data present mean ± SD, n = 3).

Treatment	IC <sub>50</sub> (μM)		RF
	SW620	AD300	
Doxorubicin solution	0.094 ± 0.018	4.796 ± 0.271	51
T0P0	0.061 ± 0.013	2.653 ± 0.125	44
T0P1	0.068 ± 0.012	2.700 ± 0.066	40
T1P0	0.073 ± 0.004	1.857 ± 0.464 <sup>b</sup>	25
T1P1	0.044 ± 0.017	1.613 ± 0.161 <sup>a</sup>	37
T1P2	0.081 ± 0.004	1.866 ± 0.082	23
T2P1	0.067 ± 0.023	1.775 ± 0.062	27
T2P2	0.074 ± 0.012	1.661 ± 0.142 <sup>c</sup>	23

IC<sub>50</sub>: concentration that inhibited cell survival by 50%.

RF: Resistance fold was the ratio of IC<sub>50</sub> value from AD300 cells over SW620 cells, respectively for all treatments.

<sup>a</sup>Statistically significant ( $p < 0.001$ ) in comparison to formulation T0P1, and.

<sup>b</sup> $p = 0.004$  in comparison to formulation T0P0.

<sup>c</sup> $p < 0.001$  in comparison to free drug, and formulation T0P0 and T0P1.

Similarly to SW620 cells, all doxorubicin-loaded PBCA-NPs formulations resulted in increased fluorescence intensity within AD300 cells (Figures 5A–G). On the other hand, as expected, no nuclei accumulation was observed, when cells were treated with free doxorubicin. Instead, the fluorescence signal was observed on the cell membranes (Figure 5H). This could be due to over-expressed P-gp on AD300 cells, which did not allow doxorubicin accumulation in the nuclei (Liao et al., 2019). In comparison, the intracellular localization of doxorubicin in AD300 cells treated with formulations T2P1 (Figure 5F), and T2P2 (Figure 5G) exhibited the highest intensity. As shown in Figure 6, formulation T2P2 exhibited the significantly higher ( $p < 0.001$ ) intensity as compared to formulations T0P1, T1P0, T1P1, T1P2 as well as free doxorubicin, indicating enhanced retention of doxorubicin within AD300 cells. These findings are in line with the inhibitory action of Tween 80 on over-expressed P-gp receptors due to the higher drug retention within AD300 cells.

### Cytotoxicity Determination to Evaluate Their P-gp and Breast Cancer Resistant Protein Efflux Transporter Inhibition Potential

The cytotoxicity profiles of doxorubicin-loaded PBCA-NPs formulations from MTT assays performed on SW620 and AD300 cell lines are illustrated in Figure 7. For the comparison of the cytotoxicity profiles, IC<sub>50</sub> values (i.e., half-maximal inhibitory concentration) were calculated and displayed in Table 2. The IC<sub>50</sub> values of free doxorubicin in SW620 and AD300 cell lines were 0.094 and 4.796 μM, respectively. Interestingly, it was observed that double-coated doxorubicin-loaded PBCA-NPs (specifically formulation T2P2) showed significantly higher ( $p < 0.001$ ) cytotoxicity than free doxorubicin, single-coated (formulation T0P1) ( $p < 0.001$ ), and un-coated (formulation T0P0) ( $p = 0.004$ ) in AD300 cell line. These results suggest that double-coated PBCA-NPs, specifically, formulation T2P2 have improved anticancer property in doxorubicin resistant AD300 cells. A

**TABLE 3 |** The IC<sub>50</sub> values calculated from cytotoxicity profiles of doxorubicin-loaded PBCA-NPs formulations from MTT assays performed on H460 and MX20 cell lines (data present mean ± SD, n = 3).

Treatment	IC <sub>50</sub> (μM)		RF
	H460	MX20	
Doxorubicin solution	0.058 ± 0.002	0.813 ± 0.014	13.9
T0P0	0.196 ± 0.012	1.574 ± 0.097	8.0
T0P1	0.173 ± 0.012	1.597 ± 0.067	9.2
T1P0	0.112 ± 0.024	0.626 ± 0.025	5.6
T1P1	0.154 ± 0.016	0.674 ± 0.013 <sup>b</sup>	4.4
T1P2	0.189 ± 0.045	0.817 ± 0.030	4.3
T2P1	0.158 ± 0.002	0.637 ± 0.011	4.0
T2P2	0.135 ± 0.023	0.653 ± 0.005 <sup>a</sup>	4.9

IC<sub>50</sub>: concentration that inhibited cell survival by 50%.

RF: Resistance fold was the ratio of IC<sub>50</sub> value from MX20 cells over H460 cells, respectively for all treatments.

<sup>a</sup>Significantly lower ( $p < 0.001$ ) in comparison to formulation T1P2, and.

<sup>b</sup> $p < 0.001$  in comparison to formulation T0P1.

trend of higher cytotoxicity with increased concentration of coating with Tween 80 was observed. This trend could be attributed to inhibition of overexpressed p-glycoprotein transmembrane receptors by Tween 80 as previously reported. On the other hand, synergistic effect on cytotoxicity in AD300 cell line was observed with double-coated doxorubicin-loaded PBCA-NPs with Tween 80 and PEG 20000. Trend analysis of the synergistic effect indicates that overcoating with PEG 20000 might aid in partial reversal of resistance, which could be attributed to folding of high molecular weight PEG (>5,000 Da) presenting a barrier comprising of conformationally random molecular chains to prevent drug efflux. This partial resistance reversal action of doxorubicin-loaded PBCA-NPs formulations was determined by calculating the resistance fold (i.e., ratio of IC<sub>50</sub> values obtained in AD300 cells to those obtained in SW620 cells). As shown in Table 2, a reduction in doxorubicin mediated resistance on AD300 cell line treated with formulation T2P2 as compared to doxorubicin solution was identified (23-fold versus 51-fold) indicating that double-coating with Tween 80 and PEG 20000 on PBCA-NPs may potentiate the sensitivity of the resistant cells towards doxorubicin. However, no significant change in IC<sub>50</sub> values was observed when SW620 cells were treated with free doxorubicin in solution or formulation T2P2. This is based on the assumption that, incorporating doxorubicin within the nanoparticle will not impact its efficacy. Since IC<sub>50</sub> is a drug related parameter, we anticipate it to be similar.

The cytotoxicity profiles of doxorubicin-loaded PBCA-NPs formulations from MTT assays performed on H460 and BCRP-overexpressed MX20 cells are shown in Figure 8. And, IC<sub>50</sub> values were calculated and compared in Table 3. The IC<sub>50</sub> values of free doxorubicin within H460 and MX20 cell lines were 0.058 and 0.813 μM, respectively. It was observed that double-coated doxorubicin-loaded PBCA-NPs (formulation T1P1) showed significantly higher ( $p < 0.001$ ) cytotoxicity (about 1-fold) than free doxorubicin in comparison to single-coated PBCA-NPs (formulation T0P1) resulting in partial reversal by about

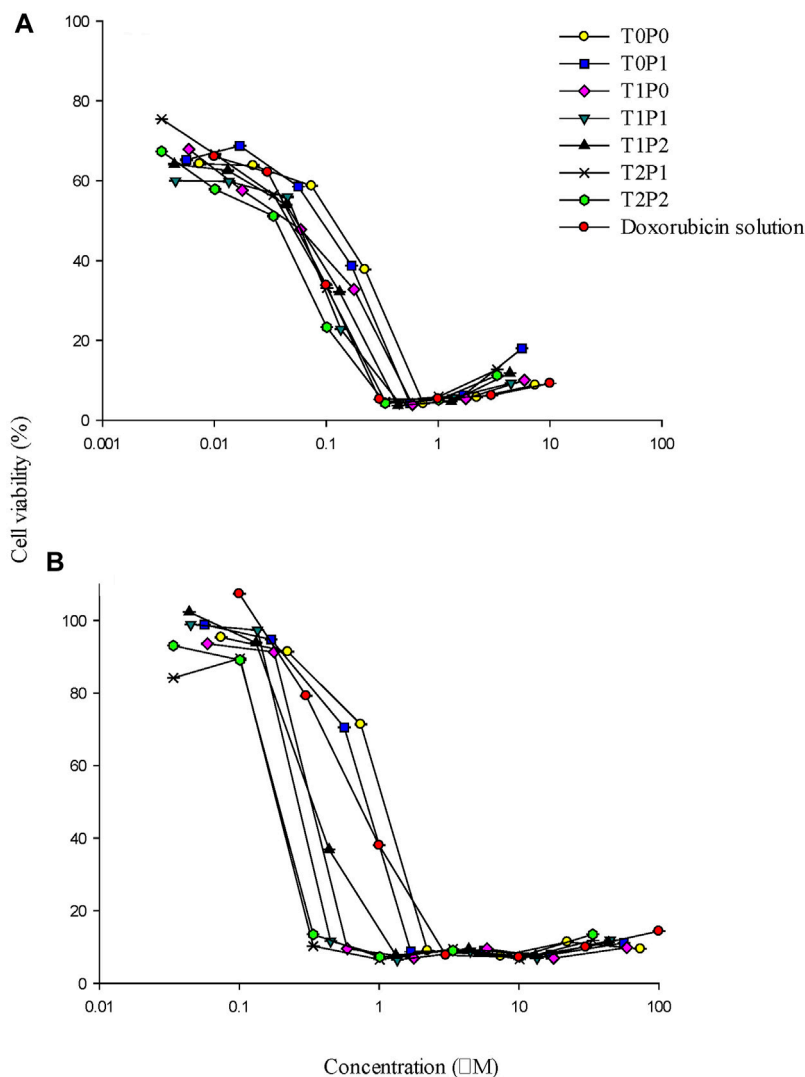


**FIGURE 8** | The cytotoxicity profiles of doxorubicin-loaded PBCA-NPs formulations from MTT assays performed on **(A)** H460 and **(B)** MX20 cell lines (data present mean  $\pm$  SD,  $n = 3$ ).

3.5-fold. These results suggest that these double-coated PBCA-NPs formulations might have improved anticancer property in mitoxantrone resistant MX20 cells. A similar trend (with respect to SW620 and AD300 cells) of higher cytotoxicity with increased concentration of overcoating with Tween 80 was observed. Consequently, formulation T2P2, exhibited significantly higher cytotoxicity in comparison to formulation T1P1. This finding suggests that an overcoat of Tween 80 at 2% might be required for enhanced cytotoxicity of formulations in resistant cells. Further, this trend could be attributed to inhibition of overexpressed BCRP transmembrane transports by Tween 80 as previously reported (Petkova et al., 2007). On the other hand,  $IC_{50}$  value of formulation T2P2 was insignificantly higher than that of formulation T1P0 (i.e., 0.653 versus 0.626), indicating similar cytotoxicity potential of formulation T2P2 as compared to

formulation T1P0. Although it may be argued, that PEG 20000 may not further enhance the cytotoxicity in mitoxantrone induced MDR cells. Overcoating with PEG 20000 may also aid in partial reversal of resistance, which could be attributed to folding of high molecular weight PEG (20,000 Da in this case) is presenting a barrier comprising of conformationally random molecular chains to prevent drug efflux (Gref et al., 2000). These results suggest that, cytotoxicity of these formulation is due to a combined effect of overcoating the nanoparticles with Tween 80 and PEG 20000. Furthermore, based on the calculated resistance fold value (**Table 3**), it can be observed that formulation T2P2 is also able to potentiate the sensitivity of doxorubicin in the mitoxantrone mediated resistant cell line (i.e., MX20), wherein the reduction of resistance from 13.9-fold (i.e., doxorubicin solution) to 4.9-fold was observed.

However, contrary to their enhanced efficacy towards the resistant cell line, lower cytotoxicity (higher IC<sub>50</sub> values) as compared to doxorubicin solution for all doxorubicin-loaded PBCA-NPs formulations was observed in H460 cell line, indicating the specificity of these formulations towards the resistant MX20 cell line. Furthermore, this difference could be attributed to variability in the availability of doxorubicin at the cellular level. For example, free doxorubicin is instantly available within the cells, whereas, with nanoparticles time dependent drug release also needs to be taken into consideration.

## CONCLUSION

In this investigation double-coated doxorubicin-loaded PBCA-NPs (formulation T2P2) could be easily prepared after the successively coating the core. The role of Tween 80 and PEG 20000 coating had been the enhancement of accumulation of doxorubicin from double-coated PBCA-NPs (formulation T2P2) in both P-gp and BCRP overexpressing cell lines. Moreover, the double-coated formulations significantly potentiated the sensitivity of doxorubicin in both P-gp and BCRP overexpressing cell lines. This reflects the transporters inhibiting action of the Tween 80 and PEG 20000. Since PEG 20000 is also known to aid in preventing the degradation of the nanoparticles. Hence, we can conclude that the double-coated PBCA-NPs with overcoats of Tween 80 and PEG 20000 represent a feasible method to deliver doxorubicin within the resistant cells.

## REFERENCES

- Chemical Society American (2020). Cancer Facts and Figures. Available at: <https://www.cancer.org/research/cancer-facts-statistics/all-cancer-facts-figures/cancer-facts-figures-2020.html>.
- Chognot, D., Six, J. L., Leonard, M., Bonneaux, F., Vigneron, C., and Dellacherie, E. (2003). Physicochemical Evaluation of PLA Nanoparticles Stabilized by Water-Soluble MPEO-PLA Block Copolymers. *J. Colloid Interf. Sci.* 268 (2), 441–447. doi:10.1016/S0021-9797(03)00591-5
- Crowley, E., McDevitt, C. A., and Callaghan, R. (2010). Generating Inhibitors of P-Glycoprotein: Where to, Now? *Methods Mol. Biol.* 596, 405–432. doi:10.1007/978-1-60761-416-6\_18
- Danaei, M., Dehghankhold, M., Ataei, S., Hasanzadeh Davarani, F., Javanmard, R., Dokhani, A., et al. (2018). Impact of Particle Size and Polydispersity Index on the Clinical Applications of Lipidic Nanocarrier Systems. *Pharmaceutics* 10 (2), 57. doi:10.3390/pharmaceutics10020057
- Das, D., and Lin, S. (2005). Double-Coated Poly (Butylcyanoacrylate) Nanoparticulate Delivery Systems for Brain Targeting of Dalargin via Oral Administration. *J. Pharm. Sci.* 94 (6), 1343–1353. doi:10.1002/jps.20357
- Duan, J., Mansour, H. M., Zhang, Y., Deng, X., Chen, Y., Wang, J., et al. (2012). Reversion of Multidrug Resistance by Co-encapsulation of Doxorubicin and Curcumin in Chitosan/Poly(Butyl Cyanoacrylate) Nanoparticles. *Int. J. Pharmaceutics* 426 (1–2), 193–201. doi:10.1016/j.ijpharm.2012.01.020
- Duffy, C., Zetterlund, P., and Aldabbagh, F. (2018). Radical Polymerization of Alkyl 2-Cyanoacrylates. *Molecules* 23 (2), 465. doi:10.3390/molecules23020465
- Gong, J., Jaiswal, R., Mathys, J.-M., Combes, V., Grau, G. E. R., and Bebawy, M. (2012). Microparticles and Their Emerging Role in Cancer Multidrug Resistance. *Cancer Treat. Rev.* 38 (3), 226–234. doi:10.1016/j.ctrv.2011.06.005

## DATA AVAILABILITY STATEMENT

The original contributions presented in the study are included in the article/**Supplementary Material**, further inquiries can be directed to the corresponding author.

## AUTHOR CONTRIBUTIONS

NK and Z-SC conceived and designed the experiments. NK performed the experiments and NK, Z-SC, and SL analyzed the data. NK wrote the paper. SL and Z-SC reviewed and made changes to the manuscript. All authors read and approved the final manuscript.

## ACKNOWLEDGMENTS

The authors acknowledge St. Johns' University for providing financial assistance and research facilities to carry out this research. We also thank Susan E. Bates and Robert W. Robey (NCI, NIH, Bethesda, MD) for providing the cell lines.

## SUPPLEMENTARY MATERIAL

The Supplementary Material for this article can be found online at: <https://www.frontiersin.org/articles/10.3389/fnano.2021.753857/full#supplementary-material>

- Gottesman, M. M., Fojo, T., and Bates, S. E. (2002). Multidrug Resistance in Cancer: Role of ATP-dependent Transporters. *Nat. Rev. Cancer* 2 (1), 48–58. doi:10.1038/nrc706
- Gref, R., Lück, M., Quellec, P., Marchand, M., Dellacherie, E., Harnisch, S., et al. (2000). 'Stealth' corona-core Nanoparticles Surface Modified by Polyethylene Glycol (PEG): Influences of the corona (PEG Chain Length and Surface Density) and of the Core Composition on Phagocytic Uptake and Plasma Protein Adsorption. *Colloids Surf. B Biointerfaces* 18 (3–4), 301–313. doi:10.1016/S0927-7765(99)00156-3
- Gulyaev, A. E., Gelperina, S. E., Skidan, I. N., Antropov, A. S., Kivman, G. Y., and Kreuter, J. (1999). Significant Transport of Doxorubicin into the Brain with Polysorbate 80-Coated Nanoparticles. *Pharm. Res.* 16 (10), 1564–1569. doi:10.1023/A:1018983904537
- Houghton, P. J., Germain, G. S., Harwood, F. C., Schuetz, J. D., Stewart, C. F., Buchdunger, E., et al. (2004). Imatinib Mesylate Is a Potent Inhibitor of the ABCG2 (BCRP) Transporter and Reverses Resistance to Topotecan and SN-38In Vitro. *Cancer Res.* 64 (7), 2333–2337. doi:10.1158/0008-5472.can-03-3344
- Jekerle, V., Klinkhammer, W., Scollard, D. A., Breitbach, K., Reilly, R. M., Piquette-Miller, M., et al. (2006). In Vitro and In Vivo Evaluation of WK-X-34, a Novel Inhibitor of P-Glycoprotein and BCRP, Using Radio Imaging Techniques. *Int. J. Cancer* 119 (2), 414–422. doi:10.1002/ijc.21827
- Jensen, E. C. (2013). Quantitative Analysis of Histological Staining and Fluorescence Using ImageJ. *Anat. Rec.* 296 (3), 378–381. doi:10.1002/ar.22641
- Kreuter, J. (1994). "Nanoparticles," in *Colloidal Drug Delivery Systems* (New York: Marcel Dekker), 277–278.
- Liao, D., Zhang, W., Gupta, P., Lei, Z.-N., Wang, J.-Q., Cai, C.-Y., et al. (2019). Tetrandrine Interaction with ABCB1 Reverses Multidrug Resistance in Cancer Cells through Competition with Anti-cancer Drugs Followed by Downregulation of ABCB1 Expression. *Molecules* 24 (23), 4383. doi:10.3390/molecules24234383

- Palmeira, A., Sousa, E., Vasconcelos, M. H., and Pinto, M. (2012). Three Decades of P-Gp Inhibitors: Skimming through Several Generations and Scaffolds. *Cmc* 19 (13), 1946–2025. doi:10.2174/092986712800167392
- Papadimitriou, S., and Bikiaris, D. (2009). Novel Self-Assembled Core-Shell Nanoparticles Based on Crystalline Amorphous Moieties of Aliphatic Copolyesters for Efficient Controlled Drug Release. *J. Controlled Release* 138 (2), 177–184. doi:10.1016/j.jconrel.2009.05.013
- Petkova, V., Benattar, J.-J., Zoonens, M., Zito, F., Popot, J.-L., Polidori, A., et al. (2007). Free-Standing Films of Fluorinated Surfactants as 2D Matrices for Organizing Detergent-Solubilized Membrane Proteins. *Langmuir* 23 (8), 4303–4309. doi:10.1021/la063249o
- Prados, J., Cabeza, L., Ortiz, R., Arias, J. L., Adolfini, M. A., Entrena, J. M., et al. (2015). Enhanced Antitumor Activity of Doxorubicin in Breast Cancer through the Use of Poly(Butylcyanoacrylate) Nanoparticles. *Ijn* 2, 1291. doi:10.2147/IJN.S74378
- Suk, J. S., Xu, Q., Kim, N., Hanes, J., and Ensign, L. M. (2016). PEGylation as a Strategy for Improving Nanoparticle-Based Drug and Gene Delivery. *Adv. Drug Deliv. Rev.* 99 (4), 28–51. doi:10.1016/j.addr.2015.09.012
- Summers, M. A., Moore, J. L., and McAuley, J. W. (2004). Use of Verapamil as a Potential P-Glycoprotein Inhibitor in a Patient with Refractory Epilepsy. *Ann. Pharmacother.* 38 (10), 1631–1634. doi:10.1345/aph.1E068
- Tejwani, R. W., Joshi, H. N., Varia, S. A., and Serajuddin, A. T. M. (2000). Study of Phase Behavior of Poly(ethylene Glycol)-Polysorbate 80 and Poly(ethylene Glycol)-Polysorbate 80-Water Mixtures. *J. Pharm. Sci.* 89 (7), 946–950. doi:10.1002/1520-6017(200007)89:7<946:AID-JPS12>3.0.CO;2-2
- Vansnick, L., Couvreur, P., Christiaens-Leyh, D., and Roland, M. (1985). Molecular Weights of Free and Drug-Loaded Nanoparticles. *Pharm. Res.* 02 (1), 36–41. doi:10.1023/A:1016366022712
- Wandel, C., Kim, R. B., Kajiji, S., Guengerich, P., Wilkinson, G. R., and Wood, A. J. (1999). P-glycoprotein and Cytochrome P-450 3A Inhibition: Dissociation of Inhibitory Potencies. *Cancer Res.* 59 (16), 3944–3948.
- Wang, X., Zhang, H., and Chen, X. (2019). Drug Resistance and Combating Drug Resistance in Cancer. *Cdr* 2, 141–160. doi:10.20517/cdr.2019.10
- Zhang, H., Yao, M., Morrison, R. A., and Chong, S. (2003). Commonly Used Surfactant, Tween 80, Improves Absorption of P-Glycoprotein Substrate, Digoxin, in Rats. *Arch. Pharm. Res.* 26 (9), 768–772. doi:10.1007/BF02976689
- Zhang, Y.-K., Zhang, G.-N., Wang, Y.-J., Patel, B. A., Talele, T. T., Yang, D.-H., et al. (2016). Bafetinib (INNO-406) Reverses Multidrug Resistance by Inhibiting the Efflux Function of ABCB1 and ABCG2 Transporters. *Sci. Rep.* 6 (1), 25694. doi:10.1038/srep25694
- Zhang, Y.-K., Zhang, H., Zhang, G.-N., Wang, Y.-J., Kathawala, R. J., Si, R., et al. (2015). Semi-Synthetic Ocotillol Analogues as Selective ABCB1-Mediated Drug Resistance Reversal Agents. *Oncotarget* 6 (27), 24277–24290. doi:10.18632/oncotarget.4493

**Conflict of Interest:** The authors declare that the research was conducted in the absence of any commercial or financial relationships that could be construed as a potential conflict of interest.

**Publisher's Note:** All claims expressed in this article are solely those of the authors and do not necessarily represent those of their affiliated organizations, or those of the publisher, the editors, and the reviewers. Any product that may be evaluated in this article, or claim that may be made by its manufacturer, is not guaranteed or endorsed by the publisher.

Copyright © 2021 Kaushal, Chen and Lin. This is an open-access article distributed under the terms of the Creative Commons Attribution License (CC BY). The use, distribution or reproduction in other forums is permitted, provided the original author(s) and the copyright owner(s) are credited and that the original publication in this journal is cited, in accordance with accepted academic practice. No use, distribution or reproduction is permitted which does not comply with these terms.